SAE TECHNICAL
PAPER SERIES

912397

Aggregation Behavior of Common Motor Oil Additives

Joseph R. Ganc and R. Nagarajan
Dept. of Chemical Engrg.
The Pennsylvania State University

The Engineering Society
For Advancing Mobility
Land Sea Air and Space®
INTERNATIONAL

International Fuels and Lubricants
Meeting and Exposition
Toronto, Canada
October 7-10, 1991

400 COMMONWEALTH DRIVE, WARRENDALE, PA 15096-0001 U.S.A.

All SAE papers, standards, and selected books are abstracted and indexed in the SAE Global Mobility Database.

ISSN 0148-7191

Printed In USA 90-1203PG

912397

Aggregation Behavior of Common Motor Oil Additives

Joseph R. Ganc and R. Nagarajan
Dept. of Chemical Engrg.
The Pennsylvania State University

Abstract

The aggregation behavior of three common motor oil additives, calcium dinonylnaphthalene sulfonate (CaDNNS), zinc dinonyldithiophosphate (ZDDP) and polyisobutenyl succinimide of tetraethylene pentamine (PIB-TEPA) in n-decane were examined using light scattering, osmometry and viscometry techniques. The experimental data were analyzed using two phenomenological models of association, the continuous association model which assumes the coexistence of aggregates of all sizes including the monomers, and the closed association model which assumes the coexistence of aggregates of only a single size with the monomers. The closed association model was found to describe the experimental data well for CaDNNS and PIB-TEPA while both association models fitted the data for ZDDP comparably, but somewhat poorly. The analysis of experimental data led to the conclusion that CaDNNS micelles were composed of 13 and 11 monomers, PIB-TEPA micelles had 19 and 9 monomers, and ZDDP aggregates had 4 and 3 monomers, at 25°C and 65°C, respectively. At 25°C, the CaDNNS and the ZDDP aggregates were ellipsoidal in shape and it was not possible to discriminate between oblate and prolate ellipsoids. The micelle sizes assuming both shapes have been estimated. The PIB-TEPA micelle was spherical with a diameter of 6.4 nm. For all three additives, the solutions were dominated by aggregates at solute concentrations larger than 0.02 gm/cm^3 (20 kg/m^3), while below this concentration, the presence of non-aggregated monomers was important to account for.

I. INTRODUCTION

Lubricants are vital to our technological world. The major component of a lubricant oil is either a petroleum derived hydrocarbon or a synthetic oil. To enhance the performance of such a base oil, effective lubricant formulations in current use incorporate a variety of additives [1,2]. A central function of additives is to decrease the oxidative and thermal degradation of base oil. Other principal functions include decreasing formation of deposits on lubricated surfaces, minimizing friction and wear, protecting against rust and corrosion, preventing direct contact between surfaces and improving the temperature dependence of the viscosity of lubricant oil. Most lubricants require the presence of more than one additive, to perform effectively. While each additive is designed for a specific purpose, its ability to perform that function is considerably altered in the presence of the other additives [3-6]. Consequently, the design of additive packages incorporating multiple components may benefit from a more fundamental understanding of the physical and chemical interactions among base oil, additives and lubricated surfaces. One area of such fundamental studies concerns the physical interactions between the various components. Of these, the interactions involving the additive and the base oil giving rise to molecular self-assembly of additives is examined in this work.

Antioxidants are additives used to prevent or reduce the oxidation of oil. A commercially important class of antioxidants is zinc dialkyl dithiophosphates, ZDDP. These molecules perform their antioxidant function by acting as peroxide decomposers. Detergent additives are used to reduce the formation of deposits in engines. The detergent additives are introduced as normal or basic salts so that any acidic product formed from the oxidative decay of base oil could be neutralized.

Further, aggregates of detergent additives can solubilize the primary oxidation products of base oil, thus removing them from contact with catalytic metal surfaces and reducing their transformation into deposits. A common detergent additive is that from the class of normal and basic salts of long chain alkyl substituted aromatic sulfonic acids, such as calcium dinonyl naphthalene sulfonate, CaDNNS. Dispersant additives refer to those which disperse sludge formed in engines operated at relatively low temperatures. Common dispersant additives include N-substituted long chain alkenyl succinic derivatives of amines, a specific example being polyisobutenyl succinimide of tetraethylene pentamine, PIB-TEPA. The molecular structures of the three types of additives mentioned above are shown in Fig.(1).

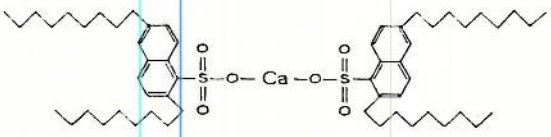

Common name: Calcium dinonyl naphthalene sulfonate (CaDNNS)

IUPAC name: Calcium 2,6-di-n-nonylnaphthalenesulfonate

CAS registry number: [57855-77-3]

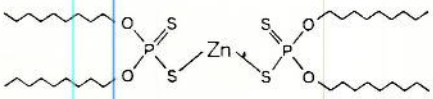

Common name: Zinc dinonyl diphosphorodithioate (ZDDP)

IUPAC name: Zinc O,O'-di-n-nonylphosphorodithioate

CAS registry number: [2457-09-2]

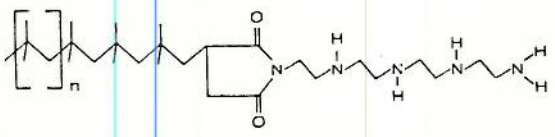

Common name: Polyisobutenyl succinimide of tetraethylene pentamine (PIB-TEPA)

IUPAC name: 3-poly(2-methylpropenyl)-1-[2-[[2-[[2-[(2-aminoethyl)amino]ethyl]amino]ethyl]amino]ethyl-2,5-pyrrolidinedione

CAS registry number: [52300-97-7] (non-polymer part only)

Figure 1. Names and structures of the three additives used in this study.

In this paper, we present experimental results on the aggregation behavior of ZDDP, CaDNNS and PIB-TEPA additives in n-decane at 25°C and 65°C based on vapor pressure osmometry, static light scattering and viscometry measurements. The experimental data obtained from the three independent techniques are all simultaneously fitted to two phenomenological models of association, namely, continuous and closed association models. From such analysis, the pattern of association, the size of the micelle as well as its shape are all determined in an integrated manner.

In the following section, the phenomenological models of association are briefly summarized. In section III, the experimental techniques are outlined. In section IV, the experimental data are interpreted in the framework of the models for molecular association. The last section presents the main conclusions.

II. PHENOMENOLOGICAL MODELS OF ASSOCIATION

Aggregation of molecules in a solution can be described by a series of stepwise reversible association reactions:

$$N_i + N_1 = N_{i+1}\,, \quad i = 1,2,3, \text{ etc.} \tag{1}$$

where, N_i refers to the number of moles per unit volume of an aggregate comprised of i monomers. The molar equilibrium constants for this reaction are defined as

$$K_{1,2} = \frac{N_2}{N_1 N_1}\,, \quad K_{2,3} = \frac{N_3}{N_1 N_2}\,, \quad K_{i,i+1} = \frac{N_{i+1}}{N_1 N_i} \tag{2}$$

The above representation is often referred to as the mass action or multiple equilibria model. This scheme does not account for possible reactions between aggregates. In general, the equilibrium constants for each of the stepwise reactions are not equal. The determination of the equilibrium constants in the above scheme differentiate one specific association model from another [7]. Two limiting representations of multiple association are discussed below.

CONTINUOUS ASSOCIATION MODEL - In this model, aggregates of all sizes are assumed to coexist and all association equilibrium constants are taken to be equal, represented by K. Consequently, eq.(1) reduces to

$$N_i = K\, N_{i-1}\, N_1 = K^{i-1} N_1^i \tag{3}$$

The number average molecular weight of the aggregate M_n is calculated from

$$M_n = M_1 \frac{\sum_{i=1}^{\infty} i N_i}{\sum_{i=1}^{\infty} N_i} = M_1 \frac{\sum_{i=1}^{\infty} i K^{i-1} N_1^i}{\sum_{i=1}^{\infty} K^{i-1} N_1^i} = M_1 \frac{1}{(1-K\,N_1)} \tag{4}$$

while the weight average molecular weight of the aggregate M_w is calculated from

$$M_w = M_1 \frac{\sum_{i=1}^{\infty} i^2 N_i}{\sum_{i=1}^{\infty} i\, N_i} = M_1 \frac{\sum_{i=1}^{\infty} i^2 K^{i-1} N_1^i}{\sum_{i=1}^{\infty} i\, K^{i-1} N_1^i} = M_1 \frac{(1+K\,N_1)}{(1-K\,N_1)} \tag{5}$$

where M_1 is the molecular weight of the monomer. From eq.(4) and (5) it is obvious that $(K\,N_1)$ cannot exceed unity. Since $(K\,N_1)$ has to be less than unity, from eq.(3) it is evident that in general, N_1 is larger than N_{i+1}. This means that the monomer is the most common i-mer based on a number basis, though not

necessarily on a weight basis. The mass concentration c of the solute is related to the total moles of monomeric units N by $c = N M_1$. It is also related to the aggregate concentrations N_i through the relation $c = \sum_{i=1}^{\infty} N_i M_i$. The total moles of the monomer per unit volume N, can be calculated by accounting for all the aggregates via

$$N = \sum_{i=1}^{\infty} i N_i = \sum_{i=1}^{\infty} i K^{i-1} N_1^i = \frac{K N_1}{K (1-K N_1)^2} \tag{6}$$

Introducing in eqs.(4) and (5) the solution for $(K N_1)$ obtained from eq.(6), one can represent the number and the weight average aggregation numbers and molecular weights in terms of c, K and M_1.

$$M_n = \frac{2cK}{\left(\frac{4cK}{M_1}+1\right)^{1/2} - 1} \tag{7}$$

$$M_w = \frac{4cK}{\left(\frac{4cK}{M_1}+1\right)^{1/2} - 1} - M_1 \tag{8}$$

The equilibrium constant K is the only parameter of the continuous association model.

CLOSED ASSOCIATION MODEL - This model assumes that aggregates of only a single size i can coexist in solution with the monomer. The association equilibrium is thus represented by

$$N_i = K^{i-1} N_1^i \tag{9}$$

where, i is allowed a single value and K^{i-1} represents the equilibrium constant for the i monomers to come together and constitute the i-mer. A characteristic feature of the closed association model is the weak dependence of i on concentration c of the additive and hence, i can be taken as practically independent of c. The number and weight average molecular weights of aggregates are obtained by averaging between the monomer and the i-mer.

$$M_n = M_1 \frac{\sum_{i=1}^{\infty} i N_i}{\sum_{i=1}^{\infty} N_i} = M_1 \frac{N_1 + i K^{i-1} N_1^i}{N_1 + K^{i-1} N_1^i} \tag{10}$$

$$M_w = M_1 \frac{\sum_{i=1}^{\infty} i^2 N_i}{\sum_{i=1}^{\infty} i N_i} = M_1 \frac{N_1 + i^2 K^{i-1} N_1^i}{N_1 + i K^{i-1} N_1^i} \tag{11}$$

The total moles N per unit volume is calculated by accounting for the i-mers and the monomers via

$$N = \sum_{i=1}^{\infty} i N_i = N_1 + i K^{i-1} N_1^i = \frac{c}{M_1} \tag{12}$$

The closed association model has thus two parameters, K and i.

PROBLEM OF POLYDISPERSED MONOMERS - In the association models described above, the monomer is taken to be one with a distinct molecular weight M_1. But lubricant additives that are chemically polymeric in nature (such as the dispersant additive PIB-TEPA) are usually mixtures of molecules of varying sizes. These polydisperse molecules, in turn, form aggregates in solution. The treatment of such a general problem has not appeared yet in the literature. For the simplifying case when the molecules can be considered to have equal propensity to form aggregates, i.e., when the composition of the aggregates and of the non-aggregated species are equivalent, a detailed analysis has been developed by Ganc [8]. The simplifying assumption of equal propensity to aggregate is almost always invalid if we consider the phenomenon of mixed micelle formation by conventional surfactants in aqueous media [9]. In these systems, the non-ideal interactions among the monomeric species and their differing tendency to form micelles in water result in the micelle composition being different from that of the monomer. However, for systems such as PIB-TEPA in n-decane, the equal propensity to aggregate may be an applicable idea. This is suggested by our theoretical analysis of the aggregation behavior of block copolymer molecules in selective solvents [10]. Our studies show that the dependence of aggregation behavior on the size of the solvent compatible block is significant, if the solvent is a very good solvent for this block. On the other hand, if the solvent is only a theta solvent for the block, the block size has only a marginal influence on the aggregation properties. For polyisobutylene, n-decane is close to a theta solvent and hence variation in the chain length of polyisobutylene may be expected to have only minor infuence on the aggregation behavior. If the polydispersity of PIB-TEPA originates from the varying lengths of the polyisobutenyl tail of the molecule that is compatible with the solvent, then molecules of different tail lengths may be considered to have equal propensity to form aggregates unaffected by the tail lengths. This is, at least, a good first approximation.

The continuous and closed association models can be rederived taking into account the polydispersity of the monomers. The analysis is non-trivial and cumbersome and hence the details are not included here; they can be found in [8]. Only the main results are summarized below. For the continuous association model, the number and weight average molecular weights of aggregates made of polydispersed monomers are given by:

$$M_n = \frac{2cK}{\left(\frac{4cK}{M_n(1)}+1\right)^{1/2} - 1} \tag{13}$$

$$M_w = \frac{4cK}{\left(\frac{4cK}{M_n(1)}+1\right)^{1/2} - 1} + M_w(1) - 2M_n(1) \tag{14}$$

In the above equations, $M_n(1)$ and $M_w(1)$ are the number and weight average molecular weights, respectively, of the polydispersed monomer. These equations replace eq.(7) and (8) in the earlier analysis of the continuous association model. Similarly, for the closed association model, the number and weight average molecular weights of the aggregates are:

$$M_n = M_n(1)\frac{N_1 + iK^{I-1}N_1^I}{N_1 + K^{I-1}N_1^I} \quad (15)$$

$$M_w = M_w(1) - M_n(1) + M_n(1)\frac{N_1 + i^2K^{I-1}N_1^I}{N_1 + iK^{I-1}N_1^I} \quad (16)$$

The total moles N per unit volume is

$$N = N_1 + iK^{I-1}N_1^I = \frac{c}{M_n(1)} \quad (17)$$

Eqs.(15) to (17) reduce to eqs.(10) to (12) when the monomers are not polydisperse and $M_n(1) = M_w(1) = M_1$. In using eq.(13) to (17) to interpret the experimental data, it should be kept in mind that these equations have been obtained from an approximate analysis for polydispersed monomers and that a more general approach remains to be developed.

III. EXPERIMENTAL STUDIES

MATERIALS - All the additives used in this work are research grade analogs of industrial motor oil additive mixtures, that is, ideally free of contaminants such as process oil and reaction intermediates. All were supplied and categorized by the kindness of the Ethyl Corporation. The impurities present in the ZDDP and CaDNNS samples were removed by dissolving the samples in spectrophotometric grade hexane, filtering, and removing the solvent in a rotary evaporator under vaccuum and moderately elevated temperature. The supplier reported that the ZDDP additive was an equal weight mixture of two different ZDDP's; the first had eight carbon atoms per hydrocarbon tail and the second had ten carbons per tail. The number and weight average molecular weights of this mixture are 824.9 and 828.7, respectively, so the polydispersity of the additive monomers is low. This additive is further treated as monodisperse. The CaDNNS additive had a molecular weight of 958 and its nonyl group was a straight hydrocarbon chain.

The PIB-TEPA sample was reported to be prepared from a polydisperse sample of polyisobutylene. The molecular weight distribution of this additive was determined by gel permeation chromatography using an analytical size exclusion column. Tetrhydrofuran (THF) was used as the eluting solvent. The column was also calibrated for molecular sizes using polystyrene standards of known molecular weights. The chromatographic analysis revealed considerable polydispersity of the sample [8]. A low molecular weight fraction (molecular weight of 79) accounted for 14.2 weight percent of the total additive. This fraction was considered to be some solvent or unreacted monomer trapped in the polymer. While the nature of this molecular specie was not identified, it was considered to be non-aggregating. Its presence was, however, taken into account in the interpretation of the experimental data. The second fraction accounting for the remaining 85.8 weight percent was identified as the polydispersed monomers of PIB-TEPA. It was determined that the number average molecular weight of the monomers $M_n(1) = 1080$ and the weight average molecular weight of the monomers $M_w(1) = 2786$. This molecular weight distribution of the monomeric PIB-TEPA additive was quantitatively taken into account in the analysis of experimental data.

The model base oil used was Humphrey's 99% n-decane. It was distilled under glass and passed through a 0.1 μm pore membrane filter before use. All other chemicals were purchased from the Aldrich Chemical Company unless otherwise noted. Solutions used in the vapor pressure osmometry experiments were prepared on a volume basis to make a concentrated solution and then diluted as needed to the desired concentrations. Solutions for all other experiments were prepared individually on a weight basis. Weight fractions were converted to mass concentrations using measured solution densities.

Density measurements were made at 25°C using the general procedure outlined by Bauer and Levin [11]. The partial molar volume of the solute and the solvent were determined using density measurements by following the procedure outlined by Shoemaker et al. [12]. It was found that the volume change on mixing the additives with n-decane were practically zero. The density, partial specific volumes and the molecular volumes are summarized in Table Ia where w is the weight fraction of the solute. Solution densities at 65°C were estimated using the partial molar volume of the solute at 25°C and the density of pure n-decane at 65°C. Details of density and partial molar volume estimations can be found in ref.[8].

Table I

Physical properties of Additives, Solvents and Solutions

(a) Volumetric Properties at 25°C

Substance	ρ [gm/cm^3]	$\hat{V}_2$ [cm^3/gm]	$\hat{V}_1$ [cm^3/gm]	V [nm^3]
n-Decane	0.7282	-	1.373	0.324
CaDNNS	0.7282 + 0.2533 w	0.902	1.373	1.437
ZDDP	0.7282 + 0.2407 w	0.921	1.371	1.267
PIB-TEPA	0.7282 + 0.1756 w	0.804	1.373	1.442

(b) Refractive Indices

Substance	$n_{25°C}$	$n_{65°C}$
n-Decane	1.4125	1.3938
Toluene	1.4976	1.4746
Decalin	1.4740	1.4565
Sample Cell	1.5140	1.5140

(c) Refractive Index Increments for Additive Solutions

Substance	$\left(\frac{\Delta n}{\Delta c}\right)_{25°C}$ [cm^3/gm]	$\left(\frac{\Delta n}{\Delta c}\right)_{65°C}$ [cm^3/gm]
CaDNNS	0.1226	0.1345
ZDDP	0.0930	0.1037
PIB-TEPA	0.1098	0.1254

VAPOR PRESSURE OSMOMETRY - Vapor pressure osmometry utilizes the difference in vapor pressure between a pure solvent and one with some solute to determine the molecular weight of that solute. A Hitatchi-Perkin-Elmer Model 115 vapor pressure osmometer was used for molecular weight determination. The experiments were run at 65°C. This high temperature was necessary for n-decane to have an appreciable vapor pressure. The osmometer was calibrated with benzil (molecular weight 210.23, Kodak Chemicals). A small amount of phosphorous pentoxide (J.T.Baker Chemicals) was placed inside the cell in contact with the vapor to remove any traces of water present in the system. The solvent and the solution were placed in different cells in close contact with thermistors. The vapor pressure difference between the two develops a steady state temperature difference which in turn leads to a difference in resistance between the thermistors. This difference in resistance ΔR was accurately measured with the use of a Wheatstone bridge. The change in resistance is related to the number average molecular weight M_n of the solute using the relation

$$\frac{\Delta R}{K_o c} = \frac{1}{M_n} + Bc \qquad (18)$$

where c is the mass concentration of the solute, K_o is an instrument constant determined by calibrating the system with a solute of known molecular weight (benzil, in this case) and B is the second virial coefficient which is a measure of any interactions between the particles.

STATIC LIGHT SCATTERING - Static light scattering utilizes the scattered light intensities of the solution and the solute free solvent to provide estimates of the weight average molecular weight of the solute. For intensity measurements, the Rayleigh ratio is defined as

$$R_\theta = \frac{r^2 I_s}{I_o} \qquad (19)$$

where I_s is the scattered light intensity, I_o is the intensity of the incident light and r is the radial distance from the light beam to the detector. The Rayleigh ratio is thus the product of scattered light intensity at some scattering angle θ and a calibration constant for the instrument. The excess Rayleigh ratio ΔR_θ for a solution is the Rayleigh ratio for the solution minus that for the pure solvent. The excess Rayleigh ratio is related to the mass concentration of the solute c, the weight average molecular weight M_w of the solute and the second virial coefficient B via the Debye equation

$$\frac{K_L c}{\Delta R_\theta} = \frac{1}{M_w} + 2Bc \qquad (20)$$

In the above equation, K_L is a constant whose magnitude is dependent on the solute and the temperature.

$$K_L = \frac{2\pi^2 n_o^2 \left(\frac{\Delta n}{\Delta c}\right)^2}{\lambda^4 N_A} \qquad (21)$$

Here, n_o is the refractive index of the solvent, λ is the wavelength of the incident light, N_A is the Avogadro's number, and $(\Delta n/\Delta c)$ is the change in refractive index with concentration for the solutions.

The light scattering experiments were performed using the commercial system developed by Brookhaven Instruments Corporation. The light source was a helium-neon laser with a nominal output of 60 mW, and the light emitted has a wavelength of 632.8 nm (short red). The sample cell made of optical quality glass was surrounded by Decalin (trade name of a mixture of cis- and trans- isomers of decahydronaphthalene) as the refractive index matching fluid. The index matching fluid could be pumped through a membrane filter to remove any dust which had contaminated the liquid. Heat transfer coils for heating or cooling were placed in close contact with the index matching fluid and were attached to a standard temperature controller.

Since the light scattering unit was not equipped to measure the transmitted intensity for a sample, the goniometer must be calibrated before being used to determine the Rayleigh ratios. The calibration liquid used was spectrophotometric grade toluene. The Rayleigh ratio for toluene at 23°C and 632.8 nm polarized light was determined by Kaye and McDaniel [13] to be 14.02×10^{-6} cm^{-1}. The instrument was generally recalibrated each time it was used for intensity measurements. This was to eliminate any possible variance of the scattered intensity with drifts in the laser's power output or the use of a different size of final aperture on the photomultiplier tube. All intensity measurements were performed at a scattering angle of 90°.

Many precautions were taken to prevent dust contamination in the samples. The samples were filtered through 0.1μm filters before solution preparation. The sample cells were cleaned in acidic and basic solutions; rinsed with distilled, deionized and filtered water; wrapped; then dried in an oven. The sample solutions were filtered through 0.2μm PTFE filters directly into the clean cells. The cells were then capped and allowed to sit for at least one day to allow any heavy contamination to sink to the bottom. This procedure improved the reproducibility of the experiments.

The analysis of the scattered intensity data requires that the refractive indices of the sample cell, index matching liquid, solvent, and calibration solvent be known. The refractive indices of the liquids were measured on a standard Bausch and Lomb Abbe-type refractometer. Refractive indices were measured at the sodium-D line (589 nm) and were corrected to 633 nm by using standard dispersion tables. The refractometer was calibrated with a glass slab of known refractive index. Indices of the liquids were measured at 25°C and 65°C. The index of refraction of the sample cells was supplied by the manufacturer. Table Ib summarizes the needed indices at 633 nm.

The change in refractive index with changing solute concentration is also required to interpret the intensity measurements. This was determined using a Brice-Phoenix type differential refractometer manufactured by the Phoenix Precision Instruments

Corporation. The detailed procedures are described in ref.[8]. The refractive index increment with changing solute concentration are summarized in Table Ic.

VISCOMETRY - Viscometric measurements can be used to obtain information on the shape of the aggregates. As will be seen later, this requires having to make certain assumptions about the nature of the solute in solution. Notwithstanding the need for such assumptions, viscometry is widely used because of its simplicity and the little expense. Also highly precise measurements can be made. A capillary viscometer was used in this work. Here, the time necessary for some volume of fluid to flow through a capillary tube is measured. This efflux time is then related to the kinematic viscosity of the fluid. A Ubbelohde type capillary viscometer, size OC was used for all viscosity measurements. The viscometer was purchased from Cannon Instruments Co., and was calibrated by the manufacturer.

Viscosities were measured at 25°C. All solutions were filtered through 0.2 μm filters before injection into the viscometer. The efflux times for the pure solvent and for all the solutions were measured. Each efflux time is converted to kinematic viscosity (η/ρ) by multiplying by the calibration constant of the viscometer. Kinematic viscosity is converted to solution viscosity η by multiplying by the solution density ρ. Specific viscosity η_{sp} was calculated for each solution using the definition $\eta_{sp} = (\eta-\eta_o)/\eta_o$, where η_o is the viscosity of the solvent.

IV. ANALYSIS OF EXPERIMENTAL DATA BASED ON ASSOCIATION MODELS

INTERPRETATION OF OSMOMETRIC AND LIGHT SCATTERING DATA - The osmometric measurements were analyzed on the basis of the continuous association model by fitting experimental data to eq.(18), taking into consideration that the number average molecular weight M_n is given by eq.(7). The two parameters, the equilibrium constant K and the virial coefficient B, were estimated in this manner. The regressions were carried out using the SAS routines (unless otherwise noted) on the IBM mainframe computer at Penn State. Similarly, the light scattering measurements were analyzed using the continuous association model by fitting the experimental data to eq.(20) and considering that the weight average molecular weight M_w is given by eq.(8). Again, the model parameters K and B were regressed as specified before. Since the same aggregation behavior is being examined by these two techniques, we also determined the parameters K and B that fit simultaneously both the osmometry and light scattering data where such data were available (at 65°C).

The closed association model involves three parameters, the number i of molecules in an aggregate, the equilibrium constant K and the virial coefficient B. The osmometric data were fitted to eq.(18) where the number average molecular weight is now given by eq.(10). Since eq.(10) is not explicitly related to the total mass concentration c of the solute, it was also necessary to take into account eq.(12) for c, in order to obtain the model parameters by regression. Along similar lines, the light scattering measurements were analyzed using the closed association model by fitting experimental data to eq.(20). In this case, the weight average molecular weight in this equation was replaced via eqs.(11) and (12). Further, both osmometric and light scattering data were simulataneously fitted to a single set of model parameters i, K and B, as well.

Estimated parameters for the continuous and closed association models based on osmometric data alone, light scattering data alone, and both data considered together are summarized in Table II. In Fig.(2) to (4), the fit of light scattering and osmometric data to the two models is shown for CaDNNS. It is clear that the closed association model is in better agreement with the experimental data. In Figs.(5) to (7), the comparison between experiments and the regressed models is shown for ZDDP. In this case both models describe the experimental data comparably, both exhibiting some deviations. Possible explanation is discussed below. Fig.(8) to (10) show how the experimental data for PIB-TEPA solutions are described by the closed and continuous association models. In this case, the closed association model describes the experimental data better than the continuous association model.

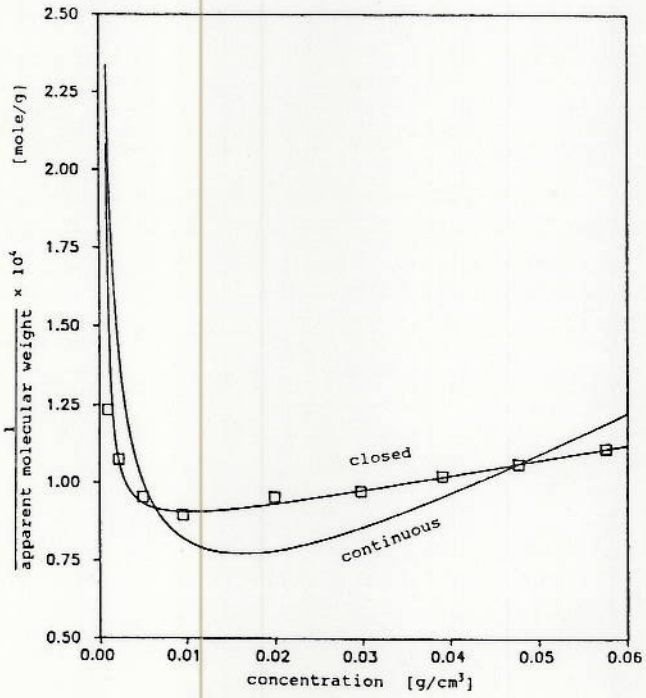

Figure 2. Fit of the continuous and closed association models to the light scattering data for CaDNNS at 25°C.

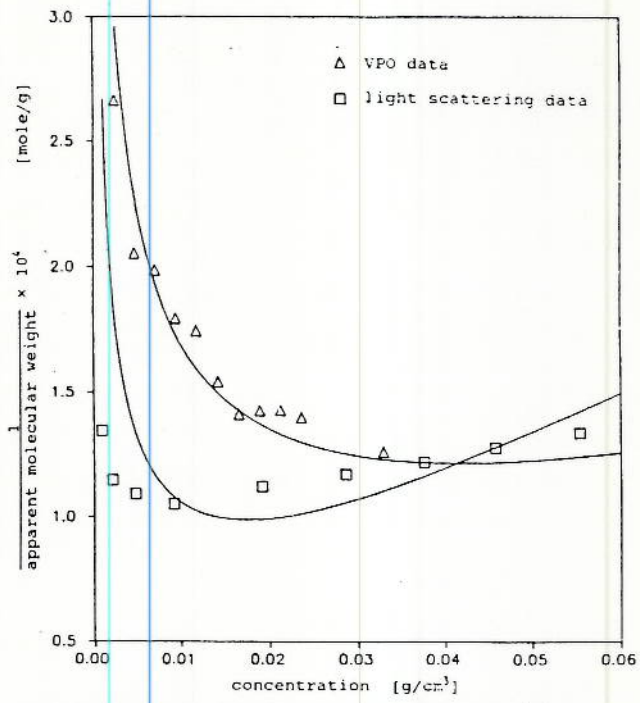

Figure 3. Fit of the continuous association model to the VPO and light scattering data for CaDNNS at 65°C.

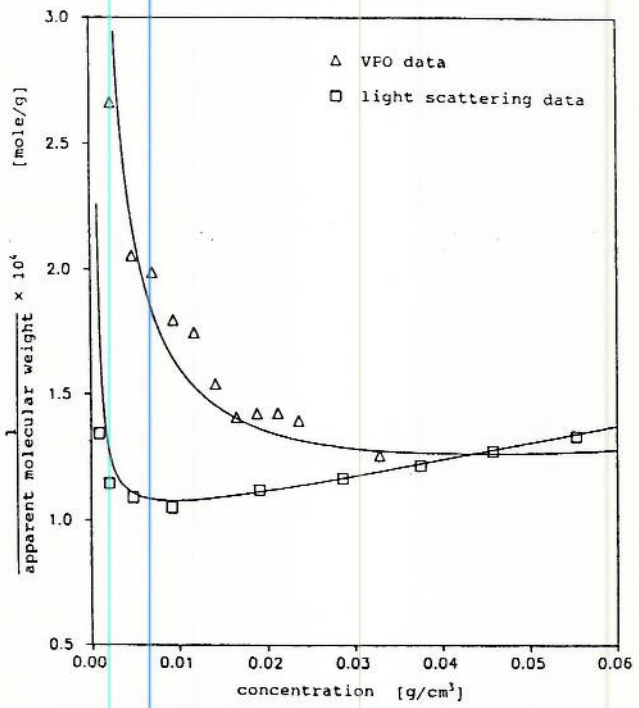

Figure 4. Fit of the closed association model to the VPO and light scattering data for CaDNNS at 65°C.

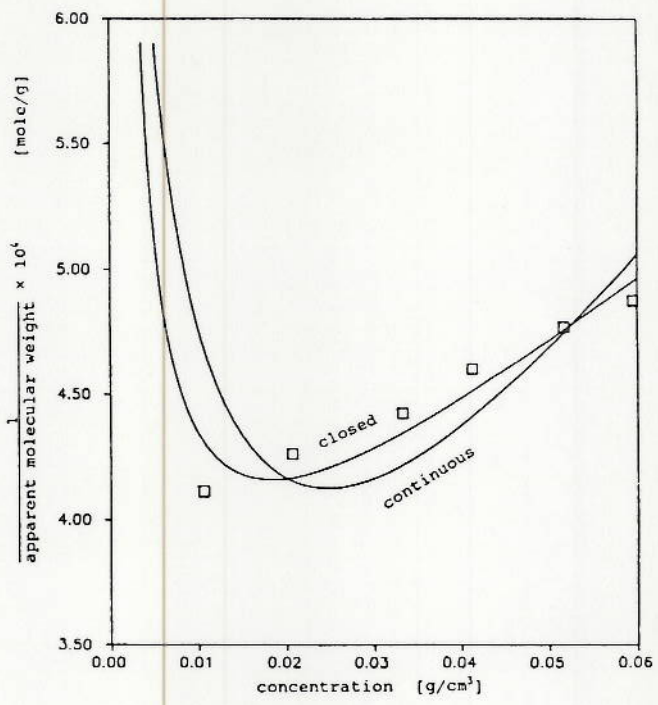

Figure 5. Fit of the continuous and closed association models to the light scattering data for ZDDP at 25°C.

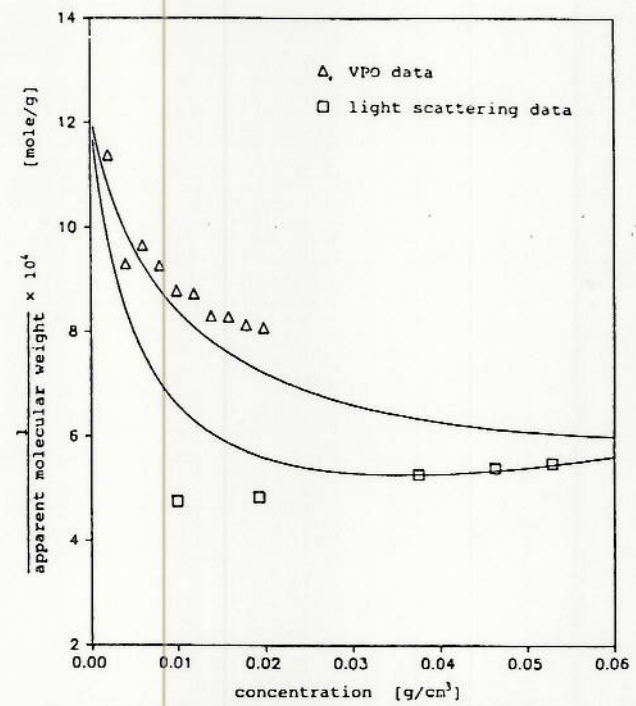

Figure 6. Fit of the continuous association model to the VPO and light scattering data for ZDDP at 65°C.

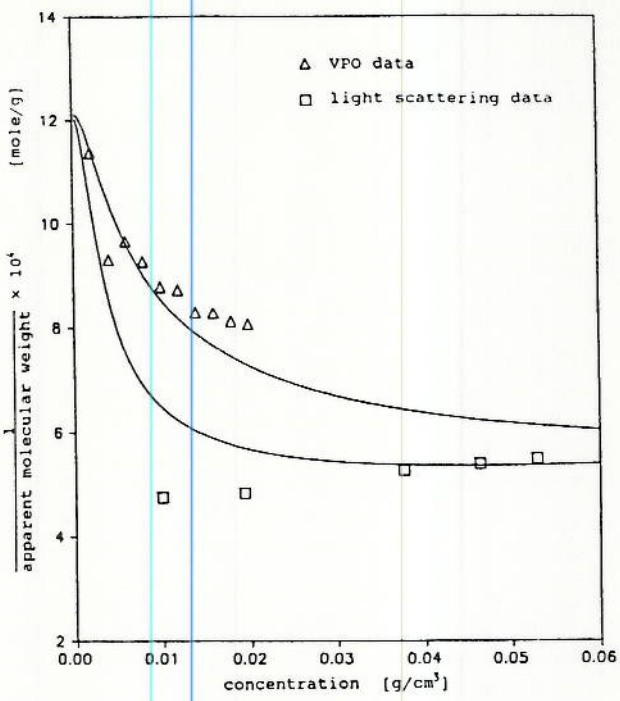

Figure 7. Fit of the closed association model to the VPO and light scattering data for ZDDP at 65°C.

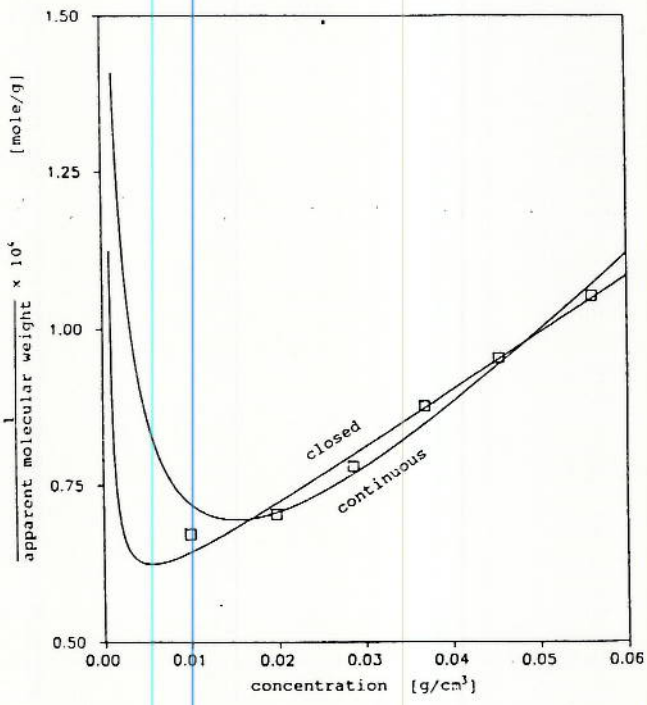

Figure 8. Fit of the continuous and closed association models to the light scattering data for PIB-TEPA at 25°C.

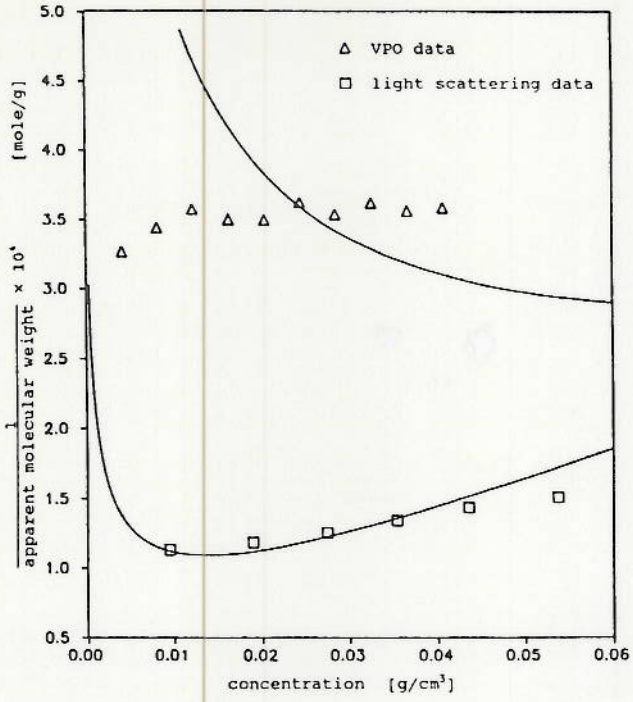

Figure 9. Fit of the continuous association model to the VPO and light scattering data for PIB-TEPA at 65°C.

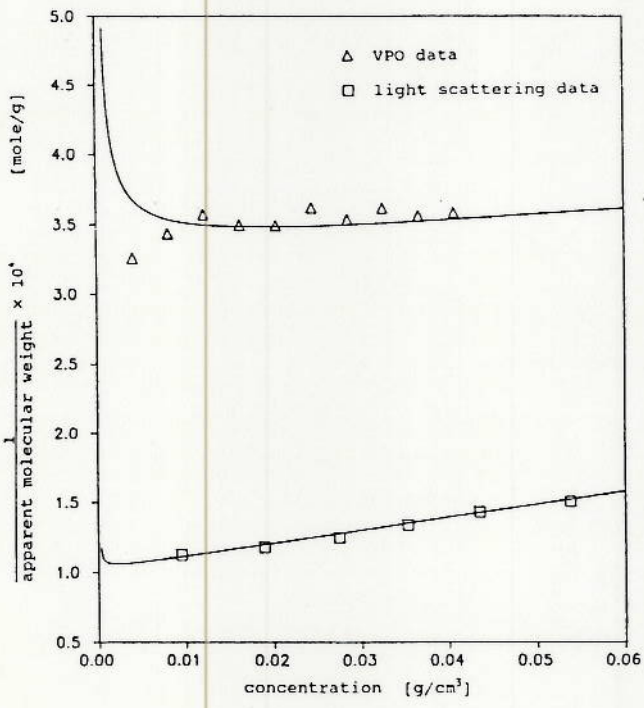

Figure 10. Fit of the closed association model to the VPO and light scattering data for PIB-TEPA at 65°C.

Table II

Fitted Association Model Parameters

System	Model	Data Type	i	K	B
				$\left(\frac{cm^3}{mole}\right)$	$\left(\frac{cm^3/gm}{gm/mole}\right)$
CaDNNS, 25 C	continuous	LS	-	6.11×10^6	0.000800
CaDNNS, 25 C	closed	LS	13	1.47×10^6	0.000260
CaDNNS, 65 C	continuous	LS	-	4.92×10^5	0.00102
CaDNNS, 65 C	continuous	VPO	-	3.58×10^5	0.00126
CaDNNS, 65 C	continuous	LS + VPO	-	3.47×10^6	0.000952
CaDNNS, 65 C	closed	LS	11	2.61×10^6	0.000346
CaDNNS, 65 C	closed	VPO	11	1.54×10^6	0.000581
CaDNNS, 65 C	closed	LS + VPO	11	1.49×10^6	0.000347
ZDDP, 25 C	continuous	LS	-	1.49×10^5	0.00270
ZDDP, 25 C	closed	LS	4	1.92×10^5	0.00142
ZDDP, 65 C	continuous	LS	-	1.22×10^5	0.00332
ZDDP, 65 C	continuous	VPO	-	6.23×10^4	0.00715
ZDDP, 65 C	continuous	LS + VPO	-	5.98×10^4	0.00233
ZDDP, 65 C	closed	LS	3	6.12×10^5	0.00126
ZDDP, 65 C	closed	VPO	3	9.76×10^4	0.00670
ZDDP, 65 C	closed	LS + VPO	3	7.93×10^4	0.00621
PIB-TEPA, 25 C	continuous	LS	-	8.01×10^6	0.000729
PIB-TEPA, 25 C	closed	LS	19	1.96×10^6	0.000464
PIB-TEPA, 65 C	continuous	LS	-	2.01×10^6	0.000975
PIB-TIBA, 65 C	continuous	VPO	-	7.36×10^5	0.00522
PIB-TIBA, 65 C	continuous	LS + VPO	-	3.20×10^6	0.00123
PIB-TIBA, 65 C	closed	LS	9	10.0×10^9	0.000453
PIB-TIBA, 65 C	closed	VPO	9	6.45×10^7	0.000749
PIB-TIBA, 65 C	closed	LS + VPO	9	2.44×10^7	0.000468

(LS - light scattering, VPO - vapor osmometry)

ELUCIDATION OF AGGREGATE SHAPE FROM VISCOMETRY - The use of viscometric data to get information about the aggregates requires assumption as to the rigidity or flexibility of the particles. In this study, the aggregates were considered to be rigid particles in solution. The specific viscosity of a solution of rigid particles when some interactions are present is given [14] by the relation

$$\eta_{sp}=\nu\phi+0.75(\nu\phi)^2 \qquad (22)$$

where ϕ is the volume fraction of the particles in solution and ν is the shape factor. The volume fraction ϕ is the product of the specific volume of the monomeric solute $\hat{V}$ and the mass concentration c, of the total monomers in solution. The shape factor ν is related to the intrinsic viscosity $[\eta]$, also via the specific volume of the solute.

$$\phi=c\hat{V}, \quad \nu=\frac{[\eta]}{\hat{V}} \qquad (23)$$

The shape factor ν for spheres is equal to 2.5, as shown by Einstein [15]. For non-spherical particles, expressions for shape factors have been developed by Simha [16] and Kuhn and Kuhn [17]. For prolate ellipsoids with semi-major axis a and semi-minor axis b, the shape factor is given by

$$\nu=2.5+0.407(a/b-1)^{1.508}, \quad 1\le a/b\le 15 \qquad (24)$$

For oblate ellipsoids, with semi-major axis b and semi-minor axis a, the shape factor is given by

$$\nu=2.5+\frac{32}{15\pi}(b/a-1)-0.628\frac{(b/a-1)}{(b/a-0.075)}, \qquad (24)$$

$$0\le a/b\le 1 \qquad (25)$$

Obviously, when a/b equals unity, the equations for prolate and oblate ellipsoids reduce to that for spheres, the shape factor being 2.5. The axial ratio a/b for any aggregate containing i monomers can be calculated from the relation between the volume and the semiaxes of the ellipsoids:

$$\frac{a}{b}=\frac{3V_1 i}{4\pi b^3} \quad \text{(prolate)}, \quad \frac{a}{b}=\frac{4\pi a^3}{3V_1 i} \quad \text{(oblate)} \qquad (26)$$

where, V_1 is the volume of a monomer molecule. In writing the above geometrical relation, we recognize that the semi-minor axis b of the prolate ellipsoid and the semi-minor axis a of the oblate ellipsoid are not modified by changing aggregation numbers. Aggregates of varying aggregation numbers differ from one another in the magnitude of their semi-major axes.

For a solution containing aggregates of various sizes, one has to take into account that aggregates of each distinct size is associated with a distinct shape factor or intrinsic viscosity. The overall solution properties are governed by a weighted average shape factor obtained as the sum of the weighted average contributions from the individual particles [14].

$$\nu=\sum_{i=1}^{\infty}\nu_i w_i, \qquad w_i=\frac{N_i M_i}{c} \qquad (27)$$

Depending upon whether the aggregates in solution are described by the continuous or closed association model, the weight fractions w_i in the above equation can be calculated using the appropriate expressions for N_1. By combining eq.(24) or (25) with eq.(27) for a solution containing aggregates, we can write expressions for the weighted average shape factor ν for the two association models and the two ellipsoidal shapes [8]. For the continuous association model, one gets

$$\nu=\frac{M_1}{Kc}\sum_{i=1}^{\infty} i\left(2.5+0.407\left(\frac{a}{b}-1\right)^{1.508}\right)\left(1-\frac{M_1}{M_n}\right)^i \qquad (28)$$

for prolate ellipsoids and

$$\nu=\frac{M_1}{Kc}\sum_{i=1}^{\infty}\left(2.5+\frac{32}{15\pi}(b/a-1)-0.628\frac{(b/a-1)}{(b/a-0.075)}\right)\left(1-\frac{M_1}{M_n}\right)^i \qquad (29)$$

for the oblate ellipsoids. The ratio a/b, in the above equations is estimated using eq.(26) while the number average molecular weight is obtained from eq.(7). Thus, given the model parameter K for the continuous association model, the only unknown in the above equations is the semi-minor axis of the aggregate which is independent of the aggregate size. The specific viscosity can be calculated by introducing eq.(28) and (29) in eq.(22). By fitting the calculated specific viscosity to the measured specific viscosity, the semi-minor axis of the aggregate can be determined. One may note that eq.(28) and (29) contain an unlimited number of terms. In practical cases, the terms in the summation are calculated until the residual terms become inconsequential.

For the closed association model, similar analysis leads to the following expressions for the weighted average shape factor:

$$\upsilon=\frac{1}{i-1}\left(2.5\left(1-\frac{M_w}{M_1}\right)+\left[2.5+0.407\left(\frac{a}{b}-1\right)^{1.506}\right]\left(\frac{M_w}{M_1}-1\right)\right) \quad (30)$$

for prolate ellipsoids and

$$\upsilon=\frac{1}{i-1}\left(2.5\left(1-\frac{M_w}{M_1}\right)+\left[2.5+\frac{32}{15\pi}(b/a-1)-0.628\frac{(b/a-1)}{(b/a-0.075)}\right]\left(\frac{M_w}{M_1}-1\right)\right) \quad (31)$$

for the oblate ellipsoids. The ratio b/a, in the above equations is estimated using eq.(26) while the weight average molecular weight is obtained from eq.(11). Thus, given the model parameters K and i for the closed association model, the only unknown in the above equations is the semi-minor axis of the aggregate. The specific viscosity can be calculated by introducing eq.(30) and (31) in eq.(22). By fitting the calculated specific viscosity to the measured specific viscosity, the semi-minor axis of the aggregate can be determined. From the quality of the fit, one can identify whether the oblate or the prolate ellipsoidal shape is preferred for the aggregates.

For aggregates that are not rigid, the viscosity data have to be analyzed differently. This is needed for the case of PIB-TEPA aggregates, since one can expect regions of the aggregate containing the polyisobutenyl tails to resemble polymer solutions. The specific viscosity as a function of the solute concentration c is described by the relation

$$\eta_{sp}=[\eta]c+k_1[\eta]^2c^2 \quad (32)$$

which is similar to eq.(22) for rigid particles. The constant k_1, is known as the Huggins coefficient and is treated as a fitted parameter. The hydrodynamic radius of the aggregate R_h is calculated from

$$R_h=\left(\frac{3[\eta]M_w}{10\pi N_A}\right)^{1/3} \quad (33)$$

The experimental specific viscosity data for PIB-TEPA solutions are fitted to eq.(32) and the magnitude of $[\eta]$ deduced from the fit is used in eq.(33) along with the weight average molecular weight of the micelle to obtain a hydrodynamic radius of the micelle.

INTERPRETATION OF VISCOMETRIC DATA - Fig.(11) shows a comparison between the experimental and fitted viscometric data for CaDNNS solutions assuming prolate spheroidal micelles. The closed association model describes the aggregation behavior much better than the continuous association model. Similar comparison is provided in Fig.(12) assuming the aggregates to be oblate ellipsoids. In this case, both association models describe the experimental data satisfactorily, the closed association model showing a

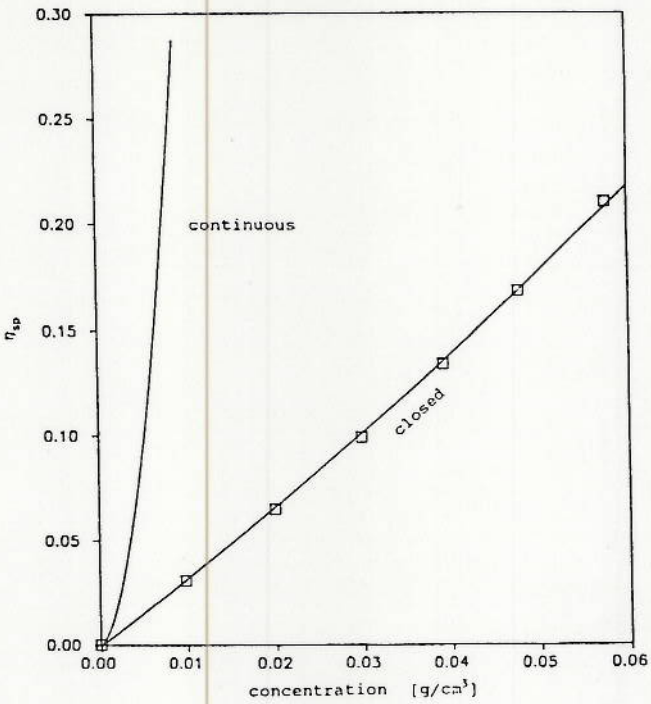

Figure 11. Fit of continuous and closed association models to the viscometric data of CaDNNS to determine the size parameters of a prolate spheroid-shaped micelle.

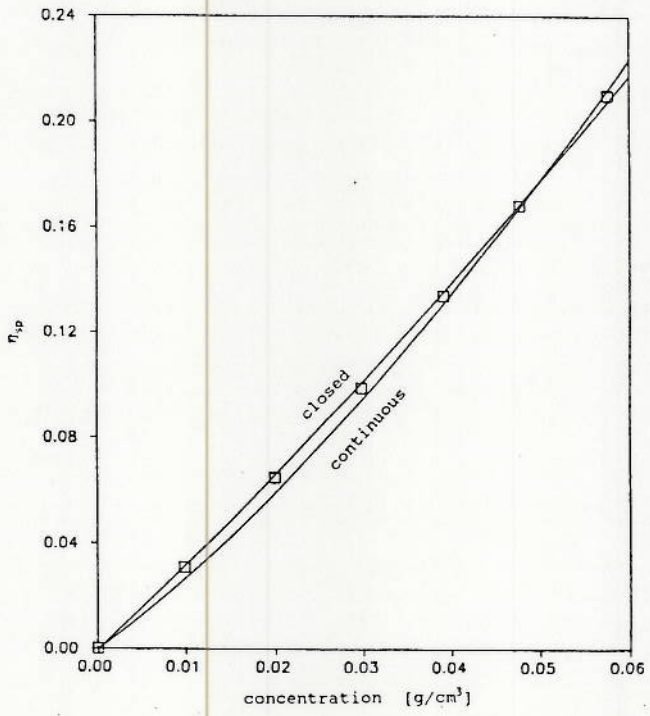

Figure 12. Fit of continuous and closed association models to the viscometric data of CaDNNS to determine the size parameters of an oblate spheroid-shaped micelle.

better fit. Thus one may conclude from viscometric data, that the closed association model better represents the aggregation behavior of CaDNNS than the continuous association model. One cannot determine, however, whether prolate or oblate ellipsoidal shape is favored. Fig.(13) and (14) present the comparison between measure-ments and fitted specific viscosities for ZDDP solutions, assuming prolate and oblate aggregates, respectively. One may observe that the closed association model is in much better agreement with measured viscosities than the continuous association model. The aggregate shape could not however be ascertained from the fitting of the viscometric data. The size parameters obtained by fitting viscometric measurements to the association models are summarized in Table III for CaDNNS and ZDDP aggregates. Fig.(15) presents a comparison between the measured and fitted specific viscosities of PIB-TEPA solutions assuming the closed association model and spherical aggregates. As mentioned earlier, the aggregates were described by equations valid for flexible polymers in solution. The parameters regressed from such a fitting show that the Huggins coefficient is different from the value of 0.75 used for rigid particles. The hydrodynamic radii were estimated to be 3.21 nm at 25°C and 2.52 nm at 65°C. These estimates were found comparable to those determined from dynamic light scattering measurements [8], not discussed in this paper. Fig.(16) to (18) depict the shapes of aggregates of CaDNNS, ZDDP and PIB-TEPA as deduced from the various experimental techniques and the models in this work. Whereas both oblate and prolate ellipsoidal shapes are consistent with viscometric data, only the oblate ellipsoidal shape for the ZDDP aggregate and the prolate ellipsoidal shape for the CaDNNS aggregate are illustrated here.

Table III

Estimated Size Parameters for Aggregates

(a) CaDNNS Micelles at 25 C

Model	Shape	a (nm)	b (nm)
continuous	prolate	-	0.70
continuous	oblate	1.05	-
closed	prolate	3.309	1.161
closed	oblate	0.764	2.416

(a) ZDDP Aggregates at 25 C

Model	Shape	a (nm)	b (nm)
continuous	prolate	-	0.671
continuous	oblate	0.77	-
closed	prolate	1.69	0.846
closed	oblate	0.649	1.365

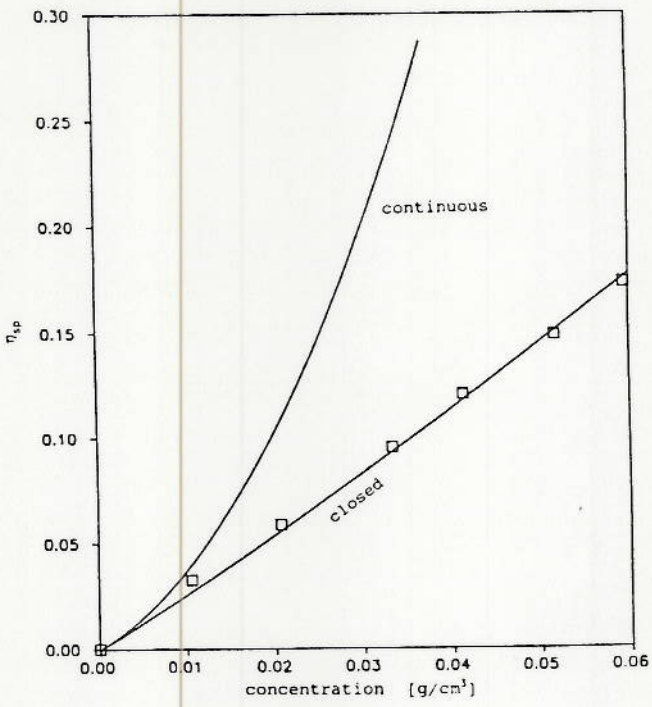

Figure 13. Fit of continuous and closed association models to the viscometric data of ZDDP to determine the size parameters of a prolate spheroid-shaped micelle.

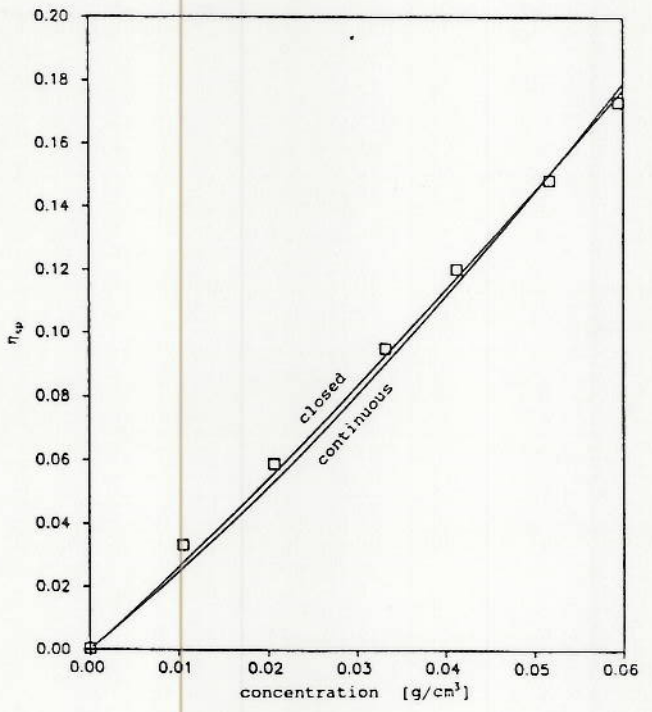

Figure 14. Fit of continuous and closed association models to the viscometric data of ZDDP to determine the size parameters of an oblate shperoid-shaped micelle.

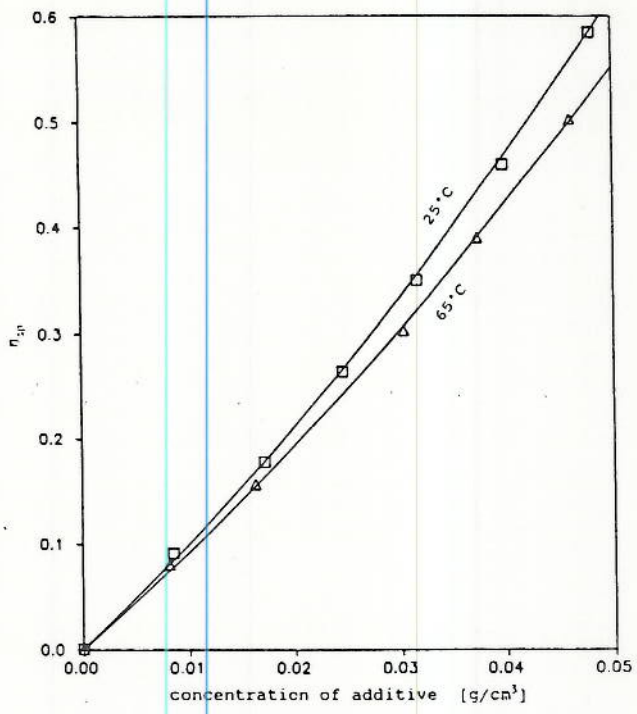

Figure 15. Fit of the closed association model to the viscometric data to determine the radius of a PIB-TEPA micelle.

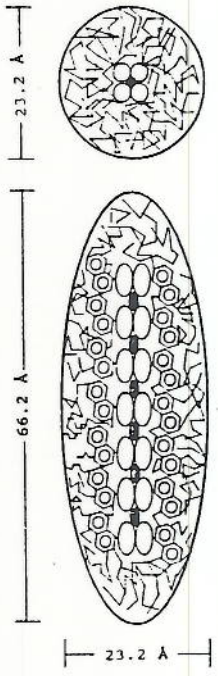

Figure 16. The size and shape of a CaDNNS micelle.

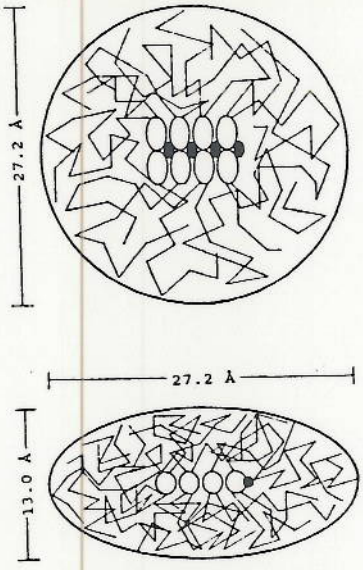

Figure 17. The size and shape of a ZDDP micelle.

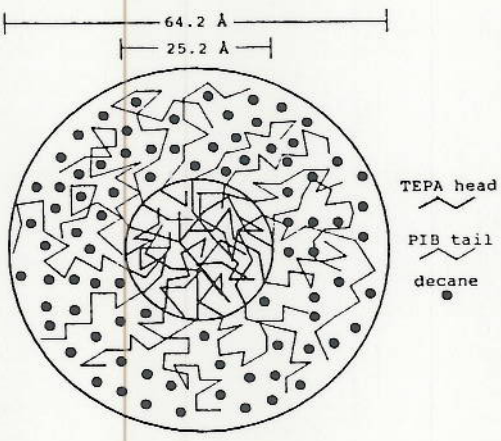

Figure 18. The size and composition of a PIB-TEPA micelle.

V. CONCLUSIONS

The aggregation behavior of calcium dinonyl naphthalene sulfonate (CaDNNS), zinc dinonyldithiophosphate (ZDDP) and polyisobutenyl succinimide of tetraethylene pentamine (PIB-TEPA) in n-decane were investigated using vapor pressure osmometry, static light scattering, and viscometry measurements. The experiments were interpreted on the basis of two well-known phenomenoloical descriptions of molecular assembly, continuous and closed association models. An important feature of this work is the consistent use of model equations to describe all experimental measurements, taking into

account the fact that the solution properties determined by the different techniques are dependent on the presence of aggregates of all sizes that are allowed as well as on the non-aggregated (or monomeric) species. From the analysis of all experimental data, it is concluded that the closed association model provides a better representation than the continuous association model for the systems considered. Also the shapes of aggregates have been suggested to be prolate or oblate ellipsoidal for CaDNNS, prolate or oblate ellipsoidal for ZDDP and spherical for PIB-TEPA. The geometrical characteristics of these aggregates have been deduced and the shapes are pictorially represented. Further, the measurements show that aggregates are dominant in solution if the solute concentrations exceed about 0.02 gm/cm^3 while the monomers are important to accout for at lower solute concentrations.

ACKNOWLEDGEMENTS

The research was supported by a grant from the Tribology program of the National Science Foundation. Dr. Steve Hsu of NIST suggested the problem area to one of the authors (RN) and Dr. Hsu and Dr. Said Jahanmir of NIST provided continued support by sharing their research results. Drs. David Wooton and Roger Sheets of the Ethyl Corporation kindly supplied the additive samples.

REFERENCES

1. C.V. Smalheer, "Additives," in Interdisciplinary Approach to Liquid Lubricant Technology, A NASA Symposium, Vol.I, 1972.

2. CRC Handbook of Lubrication, E.R.Booser, Ed., Vol.II, CRC Press, Boca Raton, Florida, 1984.

3. K.Inoue and H.Watanabe, "Interactions of Engine Oil Additives," ASLE Trans., 26, 189 (1982).

4. F.G.Rounds, "Additive Interactions and Their Effect on the Performance of a Zinc Dialkyl Dithiophosphate," ASLE Trans., 21, 91 (1978).

5. S.M.Hsu and R.S.Lin, "Interactions of Additives and Lubricating Base Oils," SAE SP 558, 61, Society of Automotive Engineers, Warrandale, PA 1983.

6. S.M.Hsu, C.S.Ku and R.S.Lin, "Relationship Between Lubricating Basestock Composition and the Effects of Additives on Oxidation Stability," SAE SP 526, 29, Society of Automotive Engineers, Warransdale, PA 1982.

7. A.S.Kertes and H.Gutmann, "The Physical Chemistry of Aggregation and Micellization," in Surface and Colloid Science, Vol.8, E.Matijevic, Ed., Wiley, New York, 1976.

8. J.R.Ganc, "A Study of the Aggregation and Micellar Behavior of Three Common Motor Oil Additives," M.S.Thesis, Department of Chemical Engineering, The Pennsylvania State University, University Park, PA 1990.

9. R.Nagarajan, "Molecular Theory for Mixed Micelles," Langmuir, 1, 331 (1985).

10. R.Nagarajan and K.Ganesh, "Block Copolymer Self-Assembly in Selective Solvents," J. Chem. Phys., 90, 5843 (1989).

11. N.Bauer and S.Z.Lewin, "Determination of Density," in Techniques of Organique Chemistry, 2nd Edition, Vol.1, A.Weissberg, Ed., Interscience Inc., New York, 1959.

12. D.P.Shoemaker, C.W.Garland, J.I.Steinfeld and J.W.Nibler, Experiments in Physical Chemistry, 4th Edition, McGraw-Hill, New York, 1981.

13. W.Kaye and J.B.McDaniel, Applied Optics, 13, 1934 (1974).

14. R.R.Matheson, "Viscosity of Solutions of Rigid Rodlike Macromolecules," Macromolecules, 13, 643 (1980).

15. A.Einstein, Investigations on the Theory of Brownian Movement, Dover Publications, New York, 1956.

16. R.Simha, J. Phys. Chem., 44, 25 (1940).

17. W.Kuhn and H.Kuhn, Helv. Chim. Acta, 28, 97 (1945).